A High-gain and WideBand Patch Antenna for 5G Millimeter-wave Applications

T. T. Truong[1,2], T.A. Vu[1,2], T. T. Do[2], D. N. Nguyen[2], D. H. T. Hoang[2], V. X. T. Nguyen[2] and M. T. Le[1,*]
[1] School of Electrical Engineering, Hanoi University of Science & Technology, Hanoi, Vietnam
[2] Viettel High Technology Industries Corporation, Hanoi, Vietnam
{themtt1, anhvt104, toandt6, nhatnd3, truyenhdhn, trungnvx}@viettel.com.vn, *Corresponding author: thuy.leminh@hust.edu.vn

***Abstract*— In this paper, we present a novel millimeter-wave antenna using the Grounded coplanar waveguide (GCPW)-to-Substrate Integrated Waveguide (SIW) transition. This high-gain and wideband antenna consists of four patches and each patch is fed by the SIW and a cross-shaped aperture. The antenna operates from 27.1 GHz to 31.9 GHz (S11 ≤ -10dB) with a peak gain of 10 dBi, and an efficiency of 89%.**

Keywords*— *Millimeter-wave (mmWave), Substrate Integrated Waveguide (SIW), Grounded Coplanar Waveguide (GCPW)-to-SIW transition, 5G.

I. INTRODUCTION

In recent years, high speed and millimeter-wave (mmWave) like 5G, 6G communications technologies have been growing rapidly. In this field, antenna plays an important component for the quality of a wireless communication system. In mmWave antennas, the choice of an appropriate transmission structure is critical for antenna performance in term of its bandwidth, efficiency and cost as well as its integration into the transceivers. There are many transmission structures with different advantages and disadvantages. Microstrip line is popular with high integration, simple structure, low cost, easy in mass production, but the loss on this kind of transmission line is not small, especially at high frequency. Rectangular waveguide (RWG) allows high energy transmission, low loss, high quality factor (Q-factor), but RWG is bulky in size and weight, so it is difficult to develop the integrated circuits with this structure. To combine the advantages of these two common types of transmission, Substrate Integrated Waveguide (SIW) technology was first introduced in [1]. To increase the flexibility of the SIW structure, the work of [2] suggested the microstrip to SIW transition and the authors of [3] proposed GCPW to SIW transition with higher efficiency and a wideband for mmWave antenna.

Beside the feeding structure, the radiator structure is very important to decide the antenna bandwidth, efficiency and radiation pattern. In 2006, the magneto-electric (ME) dipole antenna is published in [4-5] with very wide impedance bandwidth, good radiation performance, and a simple structure. Recently, the idea of the magneto-electric (ME) dipole has been persistently studied by [6-9]. All these antenna have a bandwidth of 22-50%, the maximum gain of 9.6 dBi and easy to be integrated into a printed circuit board (PCB) laminate. However, these designs still need a rectangular waveguide to feed the antenna, which are expensive and less flexible when integrated with other devices. Thereout, the works at [10-11] improved the flexibility of the antenna by using GCPW to SIW transition. However, the maximum gain of these antenna is 7 dBi over the operation bandwidth. Therefore, in this paper, we propose a high-gain patch antenna (10 dBi) with simple structure, more flexible using GCPW transmission. The proposed antenna bandwidth is 16.2% (from 27.1 GHz to 31.9 GHz) and covering the 5G mmWave band.

II. ANTENNA DESIGN

The proposed mmWave antenna is presented in Fig. 4. The antenna uses a GCPW to SIW transition to feed to four patches of radiator. The antenna design includes two main steps: GCPW to SIW transition and patch antenna equivalent with magneto-electric dipole antenna design.

A. GCPW-to-Substrate Integrated Waveguide (SIW) Transition Design

The SIW transmision is used to feed four patches of radiator to minimize the transmision loss. It consists of two rows of metal holes with diameter *d*, separated by a distance *a*, which form two electromagnetic wave walls. In each row of metal holes, holes are arranged periodically, the distance between two adjacent holes is *p*. SIW structure exhibits propagation characteristics similar to those of rectangular metallic waveguides if conditions (1)-(4) are guaranteed [12]:

$$p > d \tag{1}$$

$$0.05 < \frac{p}{\lambda_c} < 0.25 \tag{2}$$

$$p < 2d \tag{3}$$

Where, λ_c is the wavelength of cutoff frequency is calculated using the equation:

$$\lambda_c = \frac{\lambda}{\sqrt{1 - \left(\frac{\lambda}{2a_{RWG}}\right)^2}} \tag{4}$$

Where a_{RWG} is waveguide width.

However, only TE (Transverse Electric) modes can exist in SIW with the dominant mode of TE_{10}, TM (Transverse Magnetic) modes are not supported by SIW due to interruption of surface flow by the holes. The mode of propagation in the microstrip line and GCPW (Grounded coplanar waveguide) are Quasi-TEM (Quasi-Transverse Electromagnetic). In general, the transition is required to be simple, single layer. We start from the initial microstrip to SIW transition using the taper structure as in Fig. 1a, the GCPW to SIW then is proposed based on the initial transition as in Fig. 1b. The transition is designed on the Rogers 4003C (ε_r = 3.55) with the thickness *h*=0.4mm:

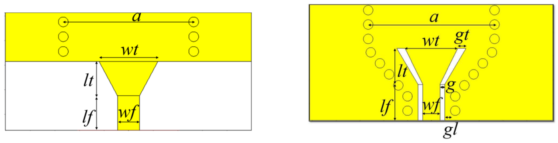

a) b)

Fig. 1: a) Initial microstrip to SIW transition b) GCPW to SIW transition

The parameters of CGPW-to-SIW transition is presented in Table 1. It is calculated using equations (5)-(8) with the length of taper *lt*= *k* λ_c */4 (k=1,3,5, 7…);*where λ_c is the wavelength of cutoff frequency. The width of taper W_t*:* is determined by solving these equations:

$$X_1 = X_2 \tag{5}$$

Where:

$$X_1 = \begin{cases} \dfrac{60}{\eta} ln\left(\dfrac{80h}{Wt} + \dfrac{0.25Wt}{h}\right) \quad if \quad \dfrac{Wt}{h} > 1 \\ \dfrac{120\pi}{\eta h\left(\dfrac{Wt}{h} + 1.393 + 0.667\, ln\left(\dfrac{Wt}{h} + 1.444\right)\right)} \\ \quad if \quad \dfrac{Wt}{h} < 1 \end{cases} \tag{6}$$

$$X_2 = \frac{4.38}{a} exp\left(-0.627 \frac{\varepsilon_r}{\dfrac{\varepsilon_r + 1}{2} + \dfrac{\varepsilon_r - 1}{2\sqrt{1 + \dfrac{12n}{Wt}}}}\right) \tag{7}$$

Where: η is the impedance wave.

In addition, the conditions of GCPW is presented in the equation (9) according to [3]:

$$wf + 2gl + 2g < \frac{c}{2f_{max}\sqrt{\varepsilon_r}} \tag{9}$$

Where *wf, g, gl* are the strip width, gap between the line and adjacent ground plane, and the distance between the gap and via. f_{max} is the maximum operating frequency.

TABLE I. PARAMETERS OF GCPW TO SIW TRANSITION

Parameters	Value (mm)	Parameters	Value (mm)
a	5.3	*wf*	0.72
g	0.2	*lt*	1.5
gt	0.65	*lf*	1.5
wt	2.2		

The transmission (S12) and reflection (S11) coefficients of the initial Microstrip-to-SIW and GCPW-to-SIW transitions are presented in Fig.2 and Fig.3. In the band from 25 GHz to 32 GHz, the S12 of GCPW-to-SIW with taper is highest showing that it this transition has the smallest loss and the maximum transmited power. The S11 of GCPW-to-SIW with taper is smallest with the peak of -70 dB (at 30 GHz) showing that GCPW-to-SIW transition has the smallest of reflected power at the GCPW input port.

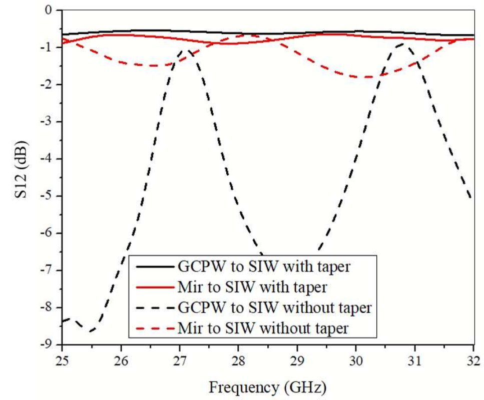

Fig. 2: S12 of Microstrip-to-SIW and GCPW-to-SIW transition with and without taper

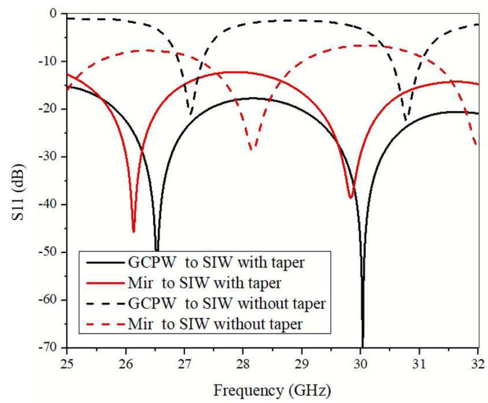

Fig. 3: S11 of Mircrostrip-to-SIW and GCPW-to-SIW transition with and without taper

B. Magneto-Electric Dipole Antenna

The geometry of the proposed high gain antenna is shown in Fig. 4. It comprises two Rogers 4003C substrate layers with a relative dielectric constant of 3.55 and the loss tangent is 0.0027. The GCPW to SIW transition and feeding part is designed in the Substrate 1 which has a thickness of 0.4 mm. A cross-shaped aperture is etched on the middle of substrate 1, which are also placed in the centre of the hole via in the Substrate 2. Each wing of the cross-shaped aperture has the distance of around quarter-wavelength at the center frequency. Since the energy in the direction of wave propagation (along the SIW structure) is stronger, the length of the vertical aperture is longer than the horizontal aperture by 0.6 mm. This ensures the balance energy between the two virtual sources for the patches. All radiator parts include four patches and four sets of V-shaped vias and enclosed in a square SIW cavity are in Substrate 2. The quantity metallic posts connected the patch to the middle metal layer (bottom layer of the substrate 2) is vertically increase by the size of the aperture in 2 different directions.The thickness of Substrate 2 is 0.8 mm. The detailed dimensions of the antenna are: *lc1=3.5 mm, wc1=1.3 mm, wp=2.2 mm, w1=1.3 mm, L1=7.4 mm*.

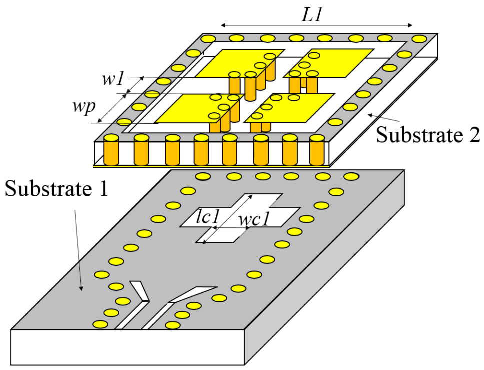

Fig. 4: Structure of the proposed antenna

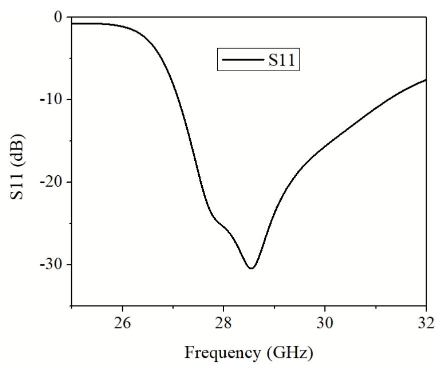

Fig. 5: Simulated S11 of the proposed antenna

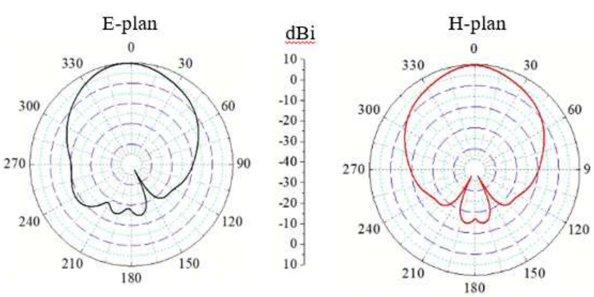

Fig. 6: a) Simulated radiation pattern (E-plan and H-plan) at 28GHz of the proposed antenna;

III. Results and Discussion

The simulated reflection coefficient of the magneto–electric dipole antenna is presented in Fig. 5, its bandwidth is 16.2% (with S11 ≤ -10 dB from 27.1 GHz to 31.9 GHz). The antenna radiation pattern is shown in Fig. 6. Fig. 7 illustrates the antenna gain and efficiency over the frequency band from 25 GHz to 32 GHz. The peak gain can reach up to 10 dBi at 28 GHz and the radiation efficiency is greater than 88% over the frequency range from 27 GHz to 32 GHz.

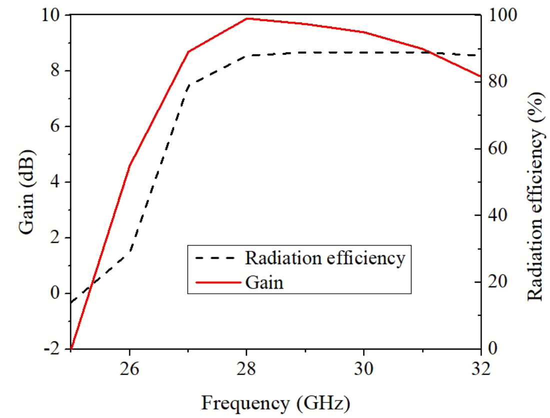

Fig. 7: Simulated realized gain and Radiation efficiency of proposed Magneto–electric dipole antenna

Current and Electric field distributions of the proposed antenna at different times are shown in Fig. 8. where T is the cycle at 28.7 GHz. As seen, at the time of t = 0 and t = T/2, the maximum of the current distribution mainly appears on the outer edge. The direction of the current and the direction of electric field are mainly along the vertical direction. Which is similar to two verticals of magneto-electric dipole antenna. At the time of t = T/4 and t = 3T/4, the direction of the current is mainly along the cross direction. This shows that the proposed patch antenna is equivalent to a pair of a cross dipoles magneto-electric dipole antenna.

Table II presents the comparison between the proposed antenna and the related antennas.

TABLE II: PERFORMANCE COMPARISON WITH THE PROPOSED ANTENNA

Ref.	Ant. Type	Feed Type (port number)	Size	Sub layers	BW (%)	Gain (dBi)	Eff. (%)
[10]	Patch	GCPW (2)	0.7 x 0.7	2	8.6	7	90
[6]	Dipole	Waveguide (2)	1x1	3	22	8.4	NA
[7]	Dipole	Waveguide (1)	1x1	2	38.7	9.4	86.9
[8]	Dipole	Waveguide (1)	1.14 x 1.14	4	36	9.6	NA
[11]	S-dipole	GCPW (1)	1x1	3	36	7	NA
[9]	Dipole	Waveguide (1)	1x1	2	50.5	9.6	95.8
[13]	Cavity-backed slot	Coaxial Cable (2)	2x2	1	9.3	9	NA
This work	Patch	GCPW (1)	1x1	2	16.2	10	89

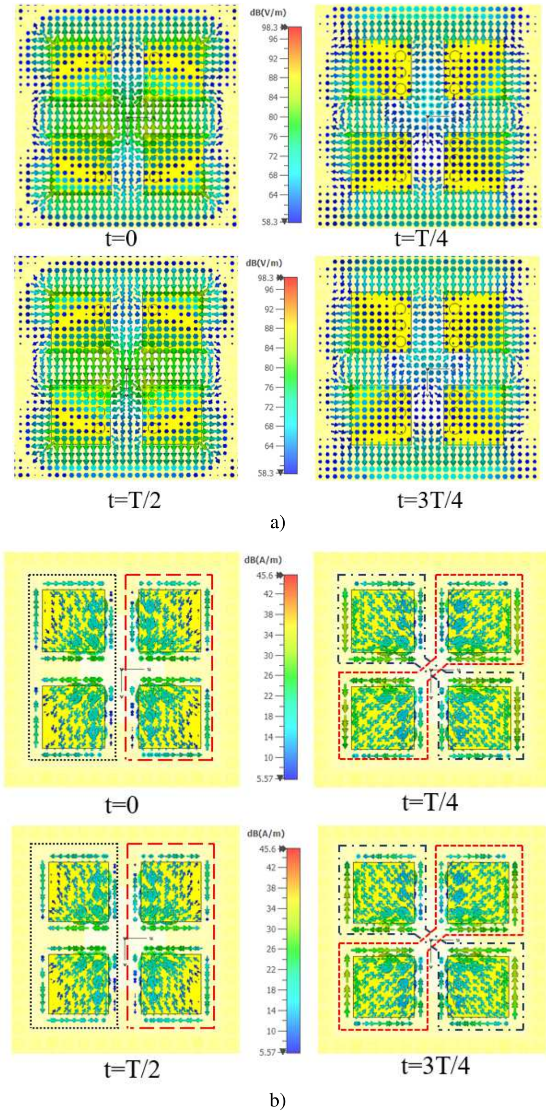

Fig. 8: Surface current distributions and E-field distributions of the proposed antenna at (a) t = 0, (b) t = T/4.

From the table II, the proposed antenna have the highest gain. The bandwidth and eficiency of the dipole antenna in [9] are highest with the same size of the propsed patch antenna and using 2 layers. However, the waveguide port is required to feed this dipole antenna making its higer cost. The patch antenna in [10] is smaller size and higer efficiency but lower gain of 3 dBi and narrower bandwidth (7.6%) compared to this work.

CONCLUSION

In this work, we proposed a high-gain patch antenna for 5G millimeter-wave application. An element antenna is designed with a bandwidth of 16.2% (at S11≤-10 dB), a peak gain of 10 dBi at 28.7GHz. The radiation efficiency is 89% at 28.7GHz. This antenna is easy to update into an array and to be integrated into transciever circuit using GCPW.

REFERENCES

[1] Ke Wu, D. Desiandes, and Y. Cassivi, “The substrate integrated circuits - a new concept for high-frequency electronics and optoelectronics,” in *6th International Conference on Telecommunications in Modern Satellite, Cable and Broadcasting Service, 2003. TELSIKS 2003.*, Serbia, Montenegro, Nis, 2003, vol. 1, p. P-III-P-X, doi: 10.1109/TELSKS.2003.1246173.

[2] D. Deslandes, “Design Equations for Tapered Microstrip-to-Substrate Integrated Waveguide Transitions,” in the 2010 IEEE MTT-S International Microwave Symposium, Anaheim, CA, USA 23-28 may, 2010, pp. 704-707, doi: 10.1109/MWSYM.2010.5517884.

[3] R. Kazemi, A. E. Fathy, S. Yang, and R. A. Sadeghzadeh, “Development of an ultra wide band GCPW to SIW transition,” in *2012 IEEE Radio and Wireless Symposium*, Santa Clara, CA, USA, Jan. 2012, pp. 171–174, doi: 10.1109/RWS.2012.6175308.

[4] B. Q. Wu and K.-M. Luk, “A Very Wideband Unidirectional Antenna Element”, in 2008 Asia Pacific Microwave Conference, Macau, Dec. 2008, pp. 1-5, doi: 10.1109/APMC.2008.4958141.

[5] Kwai-Man Luk and Biqun Wu, “The Magnetoelectric Dipole—A Wideband Antenna for Base Stations in Mobile Communications,” *Proc. IEEE*, vol. 100, no. 7, pp. 2297–2307, Jul. 2012, doi: 10.1109/JPROC.2012.2187039.

[6] Y. Li and K.-M. Luk, “60-GHz Dual-Polarized Two-Dimensional Switch-Beam Wideband Antenna Array of Aperture-Coupled Magneto-Electric Dipoles,” *IEEE Trans. Antennas Propag.*, vol. 64, no. 2, pp. 554–563, Feb. 2016, doi: 10.1109/TAP.2015.2507170.

[7] Q. Zhu, K. B. Ng, C. H. Chan, and K.-M. Luk, “Substrate-Integrated-Waveguide-Fed Array Antenna Covering 57–71 GHz Band for 5G Applications,” *IEEE Trans. Antennas Propag.*, vol. 65, no. 12, pp. 6298–6306, Dec. 2017, doi: 10.1109/TAP.2017.2723080.

[8] M. Wang, Q. Zhu, and C. H. Chan, “Wideband, Low-Profile Slot-Fed Dipole-Patch Antenna and Array,” *IEEE Antennas Wirel. Propag. Lett.*, vol. 19, no. 12, pp. 2250–2254, Dec. 2020, doi: 10.1109/LAWP.2020.3029577.

[9] Y. Li and K.-M. Luk, “A 60-GHz Wideband Circularly Polarized Aperture-Coupled Magneto-Electric Dipole Antenna Array,” *IEEE Trans. Antennas Propag.*, vol. 64, no. 4, pp. 1325–1333, Apr. 2016, doi: 10.1109/TAP.2016.2537390.

[10] Q. Yang *et al.*, “Millimeter-Wave Dual-Polarized Differentially Fed 2-D Multibeam Patch Antenna Array,” *IEEE Trans. Antennas Propag.*, vol. 68, no. 10, pp. 7007–7016, Oct. 2020, doi: 10.1109/TAP.2020.2992896.

[11] Y.-F. Wang, B. Wu, N. Zhang, Y.-T. Zhao, and T. Su, “Wideband Circularly Polarized Magneto-Electric Dipole 1x2 Antenna Array for Millimeter-Wave Applications,” *IEEE Access*, vol. 8, pp. 27516–27523, 2020, doi: 10.1109/ACCESS.2020.2971860.

[12] X.-P. Chen and K. Wu, “Substrate Integrated Waveguide Filter: Basic Design Rules and Fundamental Structure Features,” *IEEE Microw. Mag.*, vol. 15, no. 5, pp. 108–116, Jul. 2014, doi: 10.1109/MMM.2014.2321263.

[13] Kai Sun, Yanwen Zhao, Deqiang Yang, and Jin Pan "A Single-Layer Differential Substrate-Integrated Slot Antenna With Common-Mode Rejection" *IEEE antennas and wireless propagation letters*, vol. 18, pp no. 2, February 2019.